Joint Pathology Center
Veterinary Pathology Services

WEDNESDAY SLIDE CONFERENCE 2017-2018

C o n f e r e n c e 9

1 November 2017

Lauren R. Brinster, V.M.D., DACVP
NIH, Bldg. 28A, Rm. 117
9000 Rockville Pike - MSC 5230
Bethesda, MD 20892

CASE I: 17-38-W (JPC 4101294).

Signalment: 26-week-old, male, FVB/N, *Mus musculus*, mouse.

History: This mouse harbored 3 transgenes: Twist1-tetO7-luc, CCSP-rtTA, and tetO-Kras^{G12D}. The mouse had been administered doxycycline in the drinking water since 5 weeks of age to induce transgenes and promote lung tumorigenesis. The doxycycline-treated water was replaced weekly during this time. This mouse was unexpectedly found dead just prior to the intended sacrifice date.

Gross Pathology: The lungs contained numerous white-tan, firm, lung tumors that ranged from pinpoint to 3 x 3mm diameter in all lobes. Additionally, there was a 3 x 4x 0.75cm multilobulated, mass expanding the left abdominal body wall adjacent to the diaphragm (Fig 1). On cut section, the mass was composed of numerous variably sized air and blood-filled cysts. A crackling sound could be elicited upon compression of this body wall mass (subcutaneous crepitation), even post-fixation.

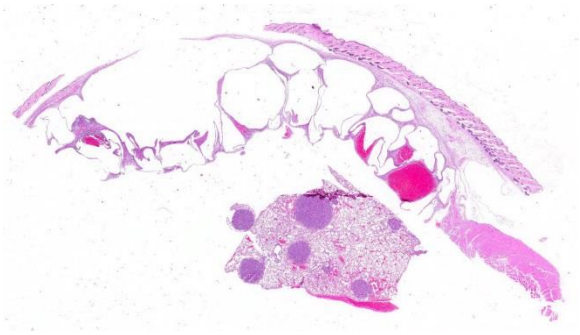

Lung and skin, mouse. The lung contains multiple nodular neoplasms within the parenchyma. The submitted section of haired skin contains numerous clear pseudocytes, some containing hemorrhage. (HE, 6X)

Laboratory results: None performed.

Microscopic Description: Lung: Compressing adjacent pulmonary parenchyma are multifocal, variably-sized, up to 3mm diameter, unencapsulated, well-demarcated, expansile, neoplastic foci composed of one or more layers of cuboidal to columnar epithelial cells arranged in

disorganized glands and packets, supported by a fine fibrovascular stroma. Neoplastic cells have variably-distinct cell borders, scant to moderate amounts of fibrillar eosinophilic to amphophilic cytoplasm, and round to oval nuclei moderately pleomorphic nuclei with finely-stippled chromatin, and 0-4 variably distinct nucleoli. The mitotic rate is less than 1 per 10 HPF. Occasionally, neoplastic cells with prominent nuclear invaginations are present. Within some neoplastic foci, there are areas of necrosis characterized by sloughed and/or pyknotic neoplastic cells, degenerative neutrophils, and cell debris. Necrotic foci are most common in the central portions of larger neoplasms. Smaller neoplastic foci can be seen extending from alveolar or bronchiolar epithelium. Within the adjacent parenchyma, alveoli often contain red blood cells and fibrin. In some sections, there are numerous alveolar macrophages containing red blood cells and/or hemosiderin.

Haired skin, body wall: Diffusely expanding the subcutis and underlying skeletal muscle, are numerous round to irregular cysts (up to 3mm in diameter) filled with clear space (air) and occasionally red blood cells, and/or inflammation and necrosis characterized by neutrophils and macrophages with fibrin and cell debris. Cystic spaces are separated by elongated collagen bundles, pre-existing skeletal muscle bundles, foci of fibroblasts, hemorrhage, and the previously described inflammation and necrosis. The skeletal muscle in this region is multifocally characterized by sarcoplasm that is pale and swollen with internalized nuclei (degeneration), or brightly eosinophilic with loss of cross striations (necrosis).

Contributor's Morphologic Diagnosis:

1. Lung: Adenocarcinoma, multifocal.
2. Haired skin and body wall: Emphysema, subcutaneous and intermuscular, with hemorrhage, and subacute myositis.

Contributor's Comment: Most human lung cancers are adenocarcinomas carrying

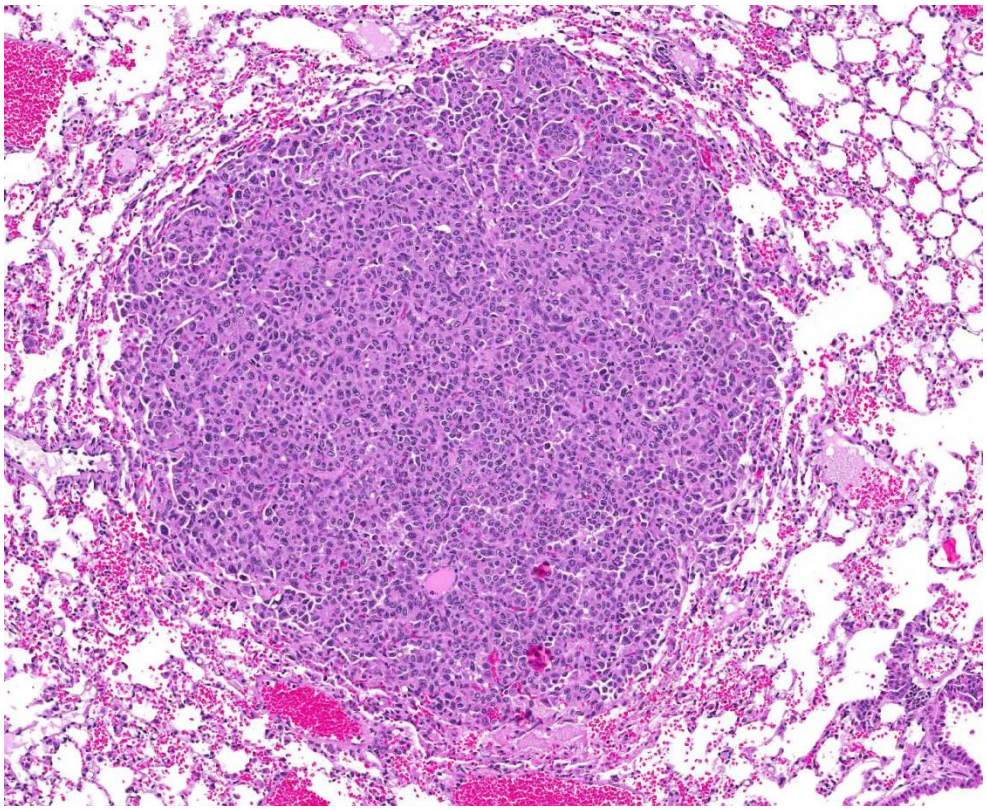

Lung, mouse. Pulmonary neoplasms are less than <3mm in diameter, and are composed of columnar epithelium which line and fill alveolar spaces, often forming papillary projections and rare glands. The neoplasms extend into, but also compress adjacent alveoli, suggesting a slow rate of growth; mitoses are rare. (HE, 112X)

somatic mutations in the genes that encode the EGFR/KRAS/BRAF pathway.[4] Mouse models utilizing the expression of these transgenes are commonly utilized as models for the human disease. Rat Clara cell secretory protein (Ccsp)-rtta activator mice were described in 2000, and provide models in which expression is conditionally controlled in respiratory epithelial cells in the lung, altering lung morphogenesis, differentiation, and proliferation.[10] Additionally, it has been shown that Twist1 plays an important role in both the acceleration and maintenance of $Kras^{G12D}$ - induced autochthonous lung tumorigenesis.[11] As can be expected based on the individual role of each of these transgenes, induction of Twist1-tetO7-luc, CCSP-rtTA, and tetO-$Kras^{G12D}$ in the mouse produces model that may be used to study tumorigenesis in human adenocarcinoma and develop potential treatments.

Subcutaneous edema is often seen in the neck, mediastinum, and retroperitoneal soft tissues secondary to trauma.[7] Additionally, it can be generated by gas forming bacteria secondary to infection or it may arise spontaneously when the pressure gradient between the air-filled alveoli and their surrounding interstitial space is sufficient to cause alveolar rupture.[7]

In this case, the emphysema developed as a bronchocutaneous fistula that presumably occurred after the rupture of one of the many adjacent lung tumors. Bronchocutaneous fistulas can occur in human lung cancer patients. They are a very rare complication, and are the extended version of a bronchopleural fistula, a direct communication between the pleura and bronchial system or the lung parenchyma.[5] Most bronchopleural fistulae are postoperative complications of surgical

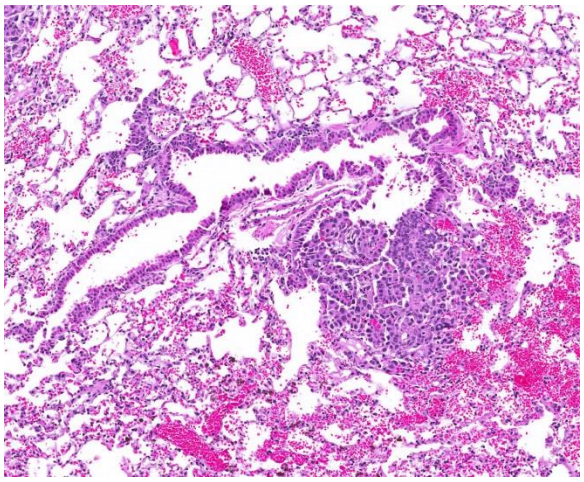

Lung, mouse. Neoplasms occasionally appear to be arising from the airway lining terminal bronchioles. (HE, 136X)

resections of lung, secondary to chemotherapy, radiation treatment, chronic inflammation or infection or a result of internal or external chest trauma.[5,8] Although rare, there are reports of bronchocutaneous fistulas developing in patients that have not received surgical resections, chemotherapy or radiotherapy.[6]

The development of numerous pulmonary adenocarcinomas was expected in the mouse, but the large area of subcutaneous emphysema in the abdominal body wall was not. This has never been described as a potential complication in an inducible lung tumor mouse models. Perhaps, with the continued use of transgenic lung tumor mouse models, rare complications like these may be seen more often by the evaluating comparative pathologists.

JPC Diagnosis: 1. Lung: Pulmonary adenomas, multiple, FVB/N (*Mus musculus)*, mouse.
2. Haired skin and subcutis: Emphysema, diffuse, subacute, severe.

Conference Comment: In mice, primary pulmonary adenomas and adenocarcinomas are the most frequent tumor. In highly susceptible strains, such as A strain mice, tumors can become apparent by 3-4 months old with 100% prevalence by 18-24 months. The high susceptibility of this strain is due to activation of K-ras in the tumors that affect their K-ras allele. In less susceptible strains such as: Outbred Swiss, FVB, BALB/c, 129, and B6:129 hybrids, a predisposition for tumor growth comes from infection with various viral infections (such as Sendai virus) or chemical carcinogens.[1] Primary pulmonary tumors are considered benign until they reach 3mm in diameter, after which they are considered adenocarcinomas or carcinomas. In this case, regardless of the mouse strain, we relied on the INHAND (International Harmonization of Nomenclature and Diagnostic Criteria for Lesions in Rats and Mice) method and determined the size of the tumors to be less than 3mm and, therefore, categorized them as adenomas.[9]

In domestic animal species, primary pulmonary neoplasms are most common in dogs and cats and epithelial tumors are the most common type. Of note, intrapulmonary metastasis is common, and therefore the presence of neoplastic cells within vessels of a pulmonary tumor is not necessarily helpful in distinguishing a primary from a secondary

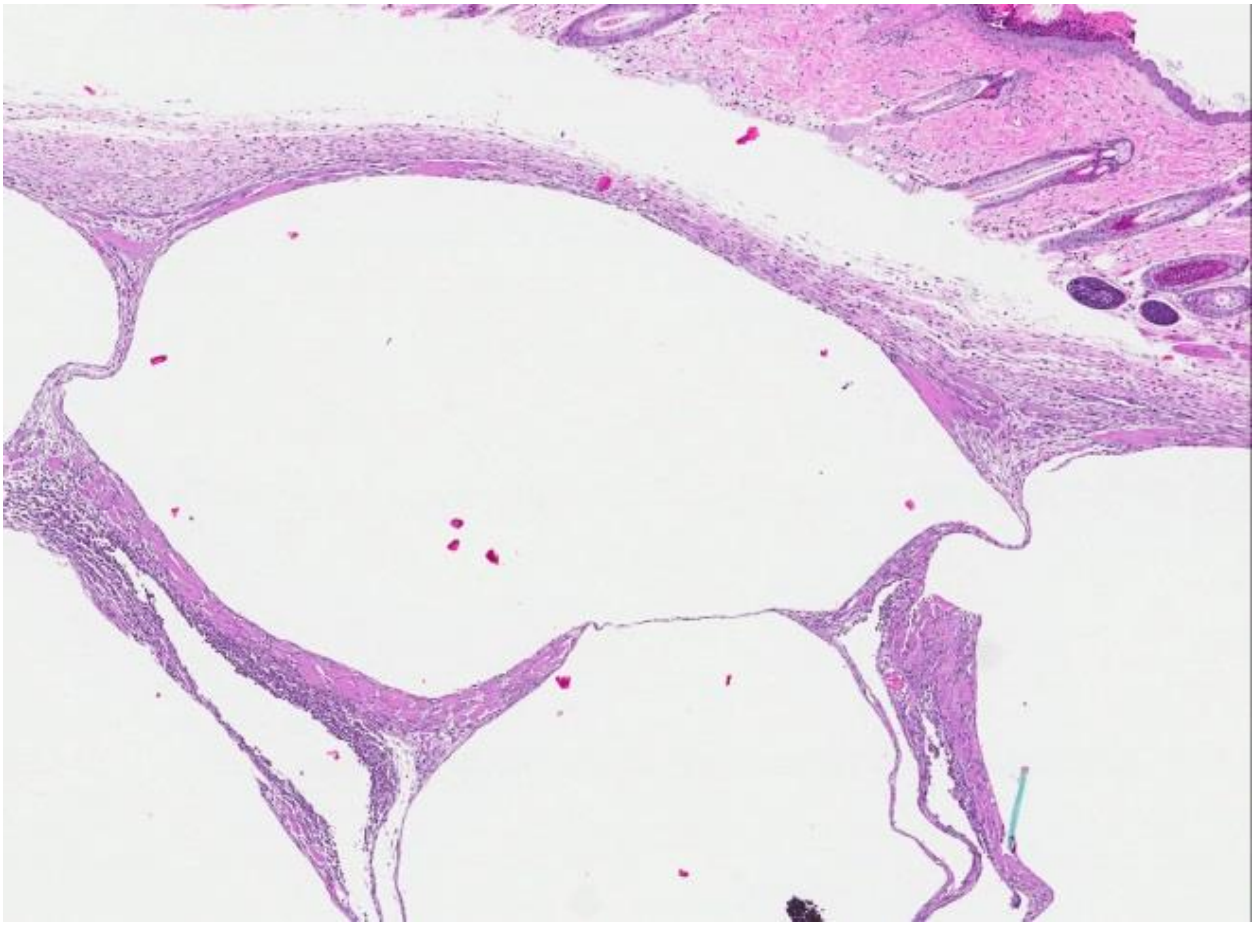

Haired skin, mouse. The dermis is expanded by large clear pseudocysts which separate the deep dermal collagen and skeletal muscle. There is a mild neutrophilic and lymphocytic infiltrate between skeletal muscle bundles reacting to degenerative changes within the muscle. (HE, 58X)

neoplasm. The histologic characteristics that support a primary neoplasm are as follows: Absence of a primary tumor in another organ, presence of single large mass with or without smaller metastases, detection of thyroid transcription factor-1 (TTF-1), mucous production or ciliated cells (both of which are rare in primary tumors).[3] Recently, a study comparing the efficacy of immunohistochemistry of surfactant protein A (SP-A), napsin A, and TTF-1 in diagnosing canine pulmonary carcinomas found that SP-A and napsin A are both useful markers, but that SP-A is the most sensitive and specific and should be paired with napsin-A or TTF-1 to improve detection and differentiation of pulmonary carcinomas from tumors metastatic to the lung.[2] The most frequent lung tumors in dogs are minimally invasive, lepidic predominant, and papillary predominant adenocarcinomas. The grading system in dogs is based on the following criteria: differentiation, degree of nuclear pleomorphism, mitotic rate, nucleolar size, tumor necrosis, fibrosis, and demarcation of the mass. The parameters most predictive of outcome are degree of differentiation, mitotic rate (cutpoints of >1 and >3 per high-power field), necrosis (> 50% of the tumor), and nucleolar size. Staging provides prognostic information, at least in dogs, and is based on number of tumors present (>1=T2), invasion of adjacent tissues (T3), or neoplastic cells present in lymph nodes or other organs (metastasis), both of which indicate a poor prognosis. With pulmonary tumors, invasion refers to neoplastic cells extending into tumor stroma, blood or lymphatic vessels, or pleura, but not extension into adjacent lung tissue. In older cats, pulmonary adenocarcinoma is quite common with a unique pattern of metastasizing to the digits, specifically the dermis on the dorsum of the distal phalanx and beneath the footpad.[3]

Contributing Institution:
Division of Laboratory Animal Resources
University of Pittsburgh
http://www.dlar.pitt.edu/

References:

1. Barthold SW, Griffey SM, Percy DH. *Pathology of Laboratory Rodents and Rabbits.* Ames, IA: John Wiley & Sons, Inc.; 2016:112-113.
2. Beck J, Miller MA, Frank C, DuSold D, et al. Surfactant protein a and napsin a in the immunohistochemical characterization of canine pulmonary carcinomas: comparison with thyroid transcription factor-1. *Veterinary Pathology*. 2017;54(5):767-774.
3. Caswell JL, Williams KJ. Respiratory system. In: Maxie MG, ed. *Jubb, Kennedy, and Palmer's Pathology of Domestic Animals*. Vol. 2. 6th ed. St. Louis, MO: Elsevier; 2016:495-497.
4. Ding L, Getz G, Wheeler DA, Mardis ER, et al. Somatic mutations affect key pathways in lung adenocarcinoma. *Nature*. 2008; 455: 1069–1075.
5. Fraser A, Nolan RL. Malignant bronchosubcutaneous fistula presenting as subcutaneous emphysema. *J Thorac Imag*. 2002; 17: 319–321.
6. Kumar A, Foden AP. Spontaneous subcutaneous emphysema secondary to a malignant bronchocutaneous fistula in a patient who had not received chemotherapy or radiotherapy. *Am J Respir Crit Care Med.* 2012; 185: A4391.
7. Maunder RJ, Pierson DJ, Hudson LD. Subcutaneous and mediastinal emphysema. Pathophysiology, diagnosis, and management. *Arch Intern Med*. 1984; 144(7): 1447-1453.
8. Powner DJ, Bierman MI. Thoracic and extrathoracic bronchial fistulas. *Chest.* 1991; 100: 480–486.

9. Renne R, Brix A, Harkema J, Herbert R, et al. Proliferative and nonproliferative lesions of the rat and mouse respiratory tract. *Toxicologic Pathology*. 2009;37(7 Suppl):5S-73S.
10. Tichelaar JW, Lu W, Whitsett JA. Conditional expression of fibroblast growth factor-7 in the developing and mature lung. *J Biol Chem*. 2000; 275(16): 11858-11864.
11. Tran PT, Shroff EH, Burns TF, Thiyagarajan S, et al. Twist1 suppresses senescence programs and thereby accelerates and maintains mutant Kras-induced lung tumorigenesis. *PLoS Genet*. 2012;8(5):e1002650.doi: 10.1371/journal.pgen.1002650.

CASE II: DX17-0022 (JPC 4101486).

Signalment: Unknown age, female, NSG mouse (NOD.*Cg-Prkdc*^{scid}*Il2rg*^{tm1Wjl}/SzJ), *Mus musculus*, mouse.

History: The mouse was part of a tumor xenograft study and was removed based on predetermined study endpoints for the pathology evaluation.

Gross Pathology: A small-sized, white firm single mass was observed within the wall of the horn of the uterus. No other gross lesions were noted at the time of necropsy.

Laboratory results:
Immunohistochemistry was performed on the mass:

MAC2: Diffuse, membranous to cytoplasmic labeling of >95% of tumor cells
CD68: Diffuse, membranous to cytoplasmic labeling of >95% of tumor cells
Lysozyme: Diffuse, cytoplasmic labeling of >95% of tumor cells
S100: Negative – diffuse, cytoplasmic labeling with blush intensity that is consistent with background; Scattered cells representing neutrophils are positively labeled
Langerin: Negative; Positive control, Haired skin: Scattered immune cells representing dendritic cells in the epidermis have positive cytoplasmic labeling
CD163: Negative; Scattered cells representing tumor infiltrating macrophages are positively labeled
CD45R/B220: Negative

Microscopic Description: An un-encapsulated, nodular mass expands a portion of the endometrium. Neoplastic cells are arranged in tight bundles and streams that are situated within a collagenous stroma. Neoplastic cells are spindle-shaped, have moderate amounts of eosinophilic cytoplasmic and have fusiform, reticulated nuclei with 1-2 prominent nucleoli. There is moderate anisocytosis and anisokaryosis. Mitoses number from 0-1 per 400x/HPF. Low numbers of neutrophils are present throughout the neoplasm. Metastatic lesions are not

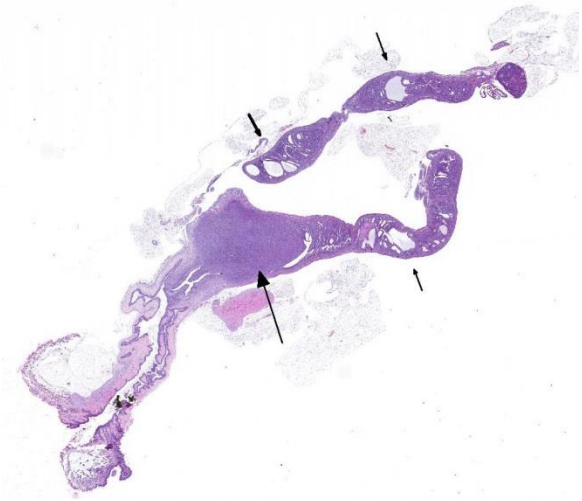

Uterus, mouse. A large mass is present at the juncture of the uterine horns and body (large arrow). The uterine horns contains multiple cysts (cystic hyperplasia) (small arrows). (HE, 6X)

observed.

Contributor's Morphologic Diagnosis: Uterus, endometrium: Histiocytic sarcoma.

Contributor's Comment: Histiocytic sarcomas arising in the uterus of laboratory mice are well-described, vary greatly in morphologic patterning, occur infrequently (~12%) and often involve other organs.[4,6] The putative cells of origin for histiocytic sarcomas for both humans and animals are considered to be CD34+ myeloid dendritic cells that have immunophenotypic characteristics of mature tissue histiocytes and possible shared clonal origins as other leukemias.[3]

In the mouse, several markers may be used to distinguish histiocytic sarcomas from other hematopoietic tumors, especially histiocyte-rich neoplasms. The markers that have shown good reproducibility by immuno-histochemistry (IHC) include: CD163, IBA1, CD68, F4/80, lysozyme and MAC2. The latter five markers are reported to be expressed by histiocytic sarcomas of variable frequency. Histiocytic sarcomas in mice and humans are frequently reported to be negative for the following lineage markers, (where applicable by species): Langerhans cell markers (e.g., Langerin/CD207, CD1A), follicular dendritic cells (CD21/CD35), T-cell related markers (e.g., CD3), common myeloid cell markers (e.g., MPO), melanocytic markers

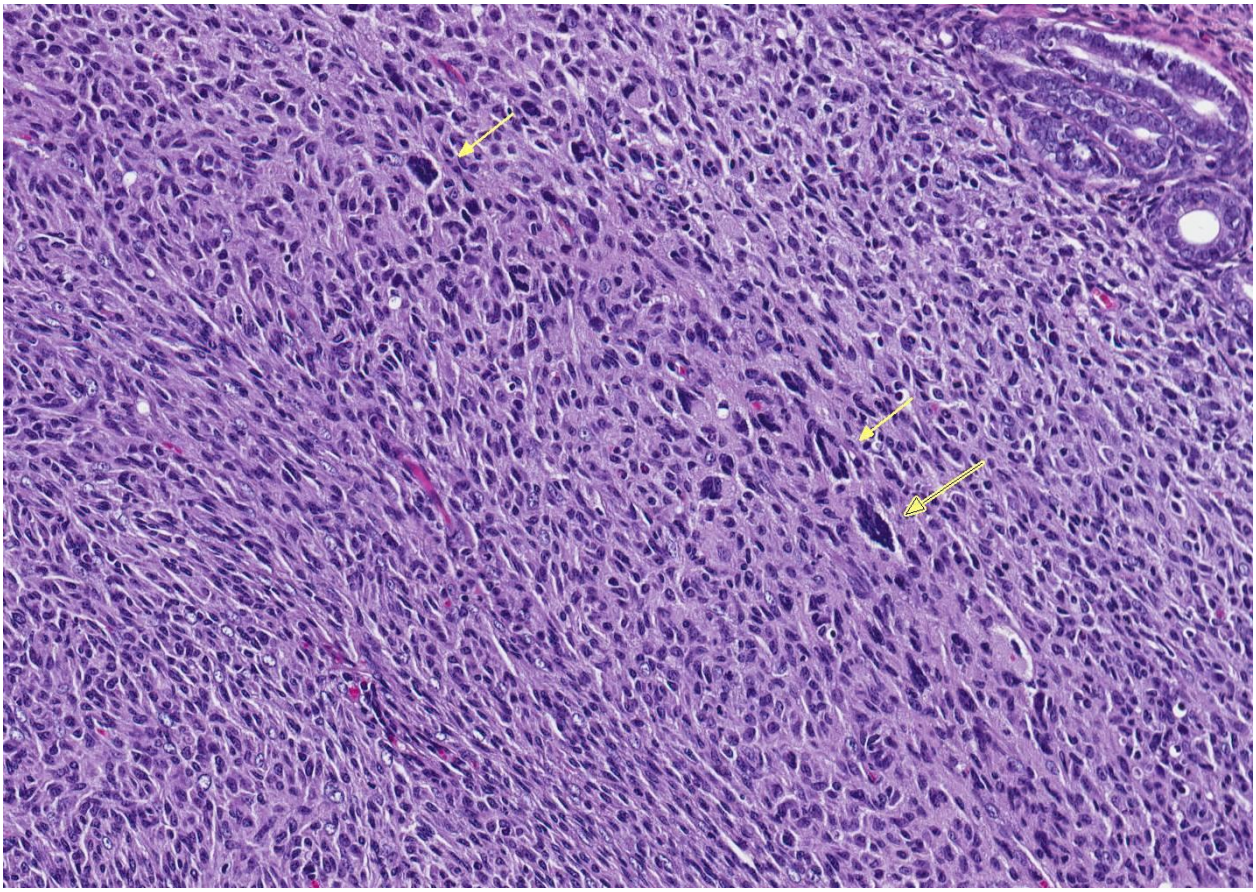

Uterus, mouse. Neoplastic cells are spindled to polygonal, and at one edge, there are low numbers of multionucleated cells, often with nuclei arranged in a ring (yellow arrows) (HE, 200X)

and epithelial cell markers.[7,8,9] The lack of CD163 expression suggests this sarcoma is not derived from tissue macrophages. However, the sarcoma expresses combinations of common histiocyte markers that may include both Langerhans and dendritic cell populations and is most consistent with tumor cells that have originated from a common bone marrow derived histiocytic progenitor.

NSG mice are deficient in mature lymphocytes and NK cells, survive beyond 16 months of age, and are relatively resistant to lymphoma development making this strain useful for long-term engraftment studies using human cells.[11] Because this strain of mouse has been developed relatively recently the incidence of spontaneously arising tumors is only starting to be documented. At least one MAC2 positive histiocytic sarcoma with multi-organ involvement has been reported.[10] Because this strain is used for engraftment studies understanding the incidence of spontaneously arising tumors, especially involving the neoplastic transformation of hematopoietic stem/progenitor cell populations is necessary for determining study related outcomes.

JPC Diagnosis: 1. Uterine body: Histiocytic sarcoma, NSG mouse (NOD.*Cg-Prkdc*^{scid}*Il2rg*^{tm1Wjl}/SzJ) (*Mus musculus)*, mouse.
2. Uterus, endometrium: Hyperplasia, cystic, diffuse, moderate.

Conference Comment: Histiocytic sarcomas (HS) arise from cells of the mononuclear-phagocytic lineage, and therefore, may be arise in any tissue of the body. Gross findings generally include enlargement of the spleen with nodular lesions in any number of additional organs (liver, uterus, vagina, kidney, lung ovaries). Neoplastic cells are large within irregular deeply basophilic nuclei, pale fibrillar cytoplasm, and fairly distinct cell borders. Often giant nuclei and multinucleated cells are present. Cells vary in "roundness" and may appear somewhat elongate, forming interlacing streams and bundles palisading along pre-existing stroma, particularly when located within the uterine wall.[1] These neoplasms are often mistaken for malignant schwannomas. In the liver, HS cells are often seen phagocytizing red blood cells (erythrophagocytosis). When HS are in lymph nodes, they are difficult to differentiate from histiocyte-associated diffuse large B-cell lymphomas and immunohistochemistry is required for definitive diagnosis. There are many markers for cells of dendritic origin (listed above) but CD18 positive membrane staining of suspected cells is diagnostic for HS.[2] Certain strains of mice (B6 and SJL) and rats (SD) are prone to HS.
An interesting associated lesion in mice is hyaline droplets within the cytoplasm of renal tubular epithelial cells which represent lysozyme released from apoptotic neoplastic histiocytes.[5] In hamsters, there has been an association noted between development of hepatic HS and *Helicobacter* spp. related hepatitis.[1]

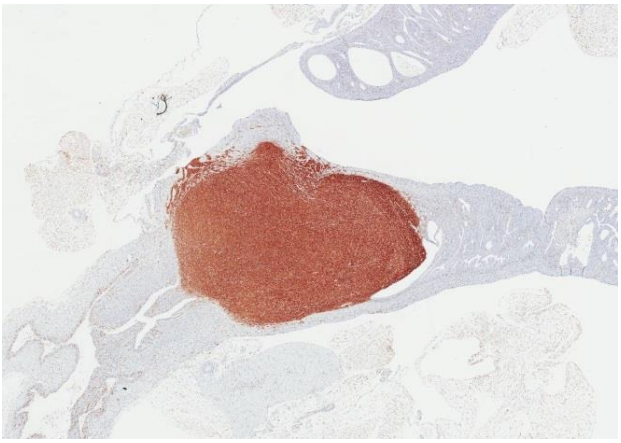

Uterus, mouse. Neoplastic cells are strongly cytoplasmically positive for MAC-2. (anti-MAC-2, 200X)

In dogs, HS are the most commonly occurring joint tumors with many breed predispositions (Bernese Mountain Dogs, Rottweilers, Bullmastiffs, golden Retrievers, Labrador Retreivers, and Flat-Coated Retrievers) as well as environmental factors that predispose such as joint damage from arthritis or ruptured cruciate ligaments. HS in dogs has a different gross appearance and is more lobulated, filling the joint cavity, and infiltrating adjacent soft tissue. Microscopically, cells have a more vacuolated cytoplasm which has led to mistaken identification as liposarcomatous neoplastic cells. Cells have a similar appearance as was previously described for rodents, but joint HS have a more favorable prognosis than those originating in the spleen.[2]

Attendees noted the cystic changes in the endometrium, and while most attendees attributed them to cystic endometrial hyperplasia - the moderator suggested that these may also simply be present as a result of compression from the mass.

The moderator also noted that NSG mice are immune-deficient, and similar to nude mice, are susceptible to hyperkeratotic skin diseases caused by *Corynebacterium*, *Staphylococcus aureus* or *S. xylosus* (ulcerative dermatitis). *C. bovis* grows within keratin due to its lipophilic nature and can persist in the environment within keratin flakes. Microscopically, they have diffuse hyperkeratosis with little dermal inflammation and gram-positive rods can be easily identified among the layers of keratin. *S. aureus* and *S. xylosus* are both commensal bacteria and are common in the environment. In immunosuppressed mice and rats, they can colonize the outer dermis and produce numerous proteins (hemolysins, nucleases, proteases, lipases, hyaluronidase, and collagenase) and exotoxins (exfoliative toxins, leukocidin, superantigens) which damage the skin and produce burn-like features.[1]

Contributing Institution:

St. Jude Children's Research Hospital
Department of Pathology
MS 250, Room 5031
262 Danny Thomas Place
Memphis, TN, 38105-3678
https://www.stjude.org/research/departments-divisions/pathology.html

References:

1. Barthold SW, Griffey SM, Percy DM. *Pathology of Laboratory Rodents and Rabbits*. Ames, IA: John Wiley & Sons, Inc.; 2016:67-70, 103, 110-111, 167-168, 183.
2. Craig LE, Dittmer KE, Thompson KG. Bones and joints. In: Maxie MG, ed. *Jubb, Kennedy, and Palmer's Pathology of Domestic Animals*. Vol. 1. 6th ed. St. Louis, MO: Elsevier; 2016:159-160.
3. Feldman AL, Minniti C, Santi M, Downing JR, Raffeld M, Jaffe ES. Histiocytic sarcoma after acute lymphoblastic leukaemia: a common clonal origin. *The Lancet Oncology*. 2004; 5(4)**:** 248-250.
4. Hao X, Fredrickson TN, Chattopadhyay SK, Han W, Qi CF, Wang Z, et al. The histopathologic and molecular basis for the diagnosis of histiocytic sarcoma and histiocyte–associated lymphoma of mice. *Veterinary Pathology*. 2010; 47(3)**:** 434-445.
5. Hard GC, Snowden RT. Hyaline droplet accumulation in rodent kidney proximal tubules: an association with histiocytic sarcoma. *Toxicologic Pathology*. 1991;19(2):88-97.
6. Lacroix-Triki M, Lacoste-Collin L, Jozan S, Charlet J-P, Caratero C,

Courtade M. Histiocytic sarcoma in C57BL/6J female mice is associated with liver hematopoiesis: review of 41 cases. *Toxicologic Pathology.* 2003; 31(3)**:** 304-309.
7. Pileri SA, Grogan TM, Harris NL, Banks P, Campo E, Chan JKC, et al. Tumours of histiocytes and accessory dendritic cells: an immunohistochemical approach to classification from the International Lymphoma Study Group based on 61 cases. *Histopathology.* 2002; 41(1)**:** 1-29.
8. Rehg JE, Bush D, Ward JM: The utility of immunohistochemistry for the identification of hematopoietic and lymphoid cells in normal tissues and interpretation of proliferative and inflammatory lesions of mice and rats. *Toxicologic Pathology.* 2012; 40(2)**:** 345-374.
9. Rehg JE, Ward JM. Applications of immunohistochemistry-toxicologic pathology of the hematolymphoid system, In: Parker G, ed. *Immunopathology in Toxicology and Drug Development: Volume 1, Immunobiology, Investigative Techniques, and Special Studies.* 1st ed. Cham, Switzerland: Humana Press; 2017: 489-551.
10. Santagostino SF, Arbona RJR, Nashat MA, White JR: Pathology of aging in NOD scid gamma female mice. *Veterinary Pathology.* 2017; 54(5): 855-869.
11. Shultz LD, Lyons BL, Burzenski LM, Gott B et al.: Human lymphoid and myeloid cell development in NOD/LtSz-scid IL2R γ null mice engrafted with mobilized human hemopoietic stem cells. *The Journal of Immunology.* 2005; 174(10)**:** 6477-6489.

CASE III: MS 15-2723 (JPC 4103775).

Signalment: 2-month-old, female, Swiss Webster, *Mus musculus*, mouse.

History: Mouse observed to have severe head tilt to the right and rolling in bedding.

Gross Pathology: A small-sized, white firm single mass was observed within the wall of the horn of the uterus. No other gross lesions were noted at the time of necropsy.

Laboratory results: None submitted.

Microscopic Description: Liver (multiple sections submitted) – Multifocal to coalescing, peri-portal to portal accumulations of one to multiple larvated parasitic eggs (live, dead, fragmented, egg casing only) surrounded by numerous layers of macrophages, and an outer layer of fibrosis with moderate numbers of neutrophils, eosinophils, and occasional plasma cells and lymphocytes are observed. A rare egg is observed attached to the endothelial lining of a portal vein along with an attached granuloma. Numerous black pigment-laden Kupffer cells (hemozoin) and multiple small accumulations of extra-medullary hematopoiesis are observed.

Liver, mouse. At low magnification, approximately 66% of the parenchyma is replaced by discrete, occasionally coalescing granulomas. (HE, 5X)

Contributor's Morphologic Diagnosis: Liver, hepatitis, periportal and portal, granulomatous to pyogranulomatous and eosinophilic, multifocal to coalescing, severe, chronic with multiple parasitic eggs consistent with Schistosomes.

Contributor's Comment:
Schistosomiasis affects more than 230 million people worldwide[2]. *S japonicum* infects a wide range of mammalian host including dogs, pigs and cattle. *S. mansoni* can infect rodents and non-human primates[2]. Schistosomiasis, also known as bilharzia/bilharziasis, is a disease caused by the trematode *Schistosoma*, with *S. mansoni*, *S. japonicum*, and *S. haematobium* being the most prevalent. Schistosomes, usually referred to as blood flukes, are part of the phylum *Platyhelminthes* (flatworms), Class *Trematoda*, and family *Schistosomatidae*. *Schistosoma*, or split body, refers to the appearance of the adult male's lateral edges that fold to form a groove (gynecophoral canal) where the female worm resides. Schistosomes differ from other trematodes in that there are distinct male and female adult worms. *S. haematobium* affects the urogenital tract, while the other two are hepatobiliary and intestinal parasites.[3]

A cercaria is a free-living, actively swimming stage, with a body and a tail. The body contains the acetabulum (ventral sucker); the tail serves to propel, and act as a fulcrum when trying to enter into the skin of a definitive host. Fatty acids (i.e; linoleic acid) and amino acids (i.e; arginine) are chemoattractants to the cercariae.

The cercariae will search for surface skin irregularities associated with hairs, ridges or wrinkles. Once attached to the host, they secrete proteolytic penetrating enzymes by the acetabulum glands; upon entering the skin, the tail detaches and they become known as schistosomules (schistosomulum). At this point, the parasite has changed morphologically and resides in the skin from one to several days before entering the dermal vasculature, after which they begin to feed and mature into the the adult worm stage. Sexes can then be distinguished. Interestingly, the male can develop fully without the female, but the female does not reach sexual maturity in the absence of the male. The female must lie within the male's gynecophoral canal for physical and reproductive development. It is believed the adult worms copulate in the liver before migrating to the mesenteric vein.

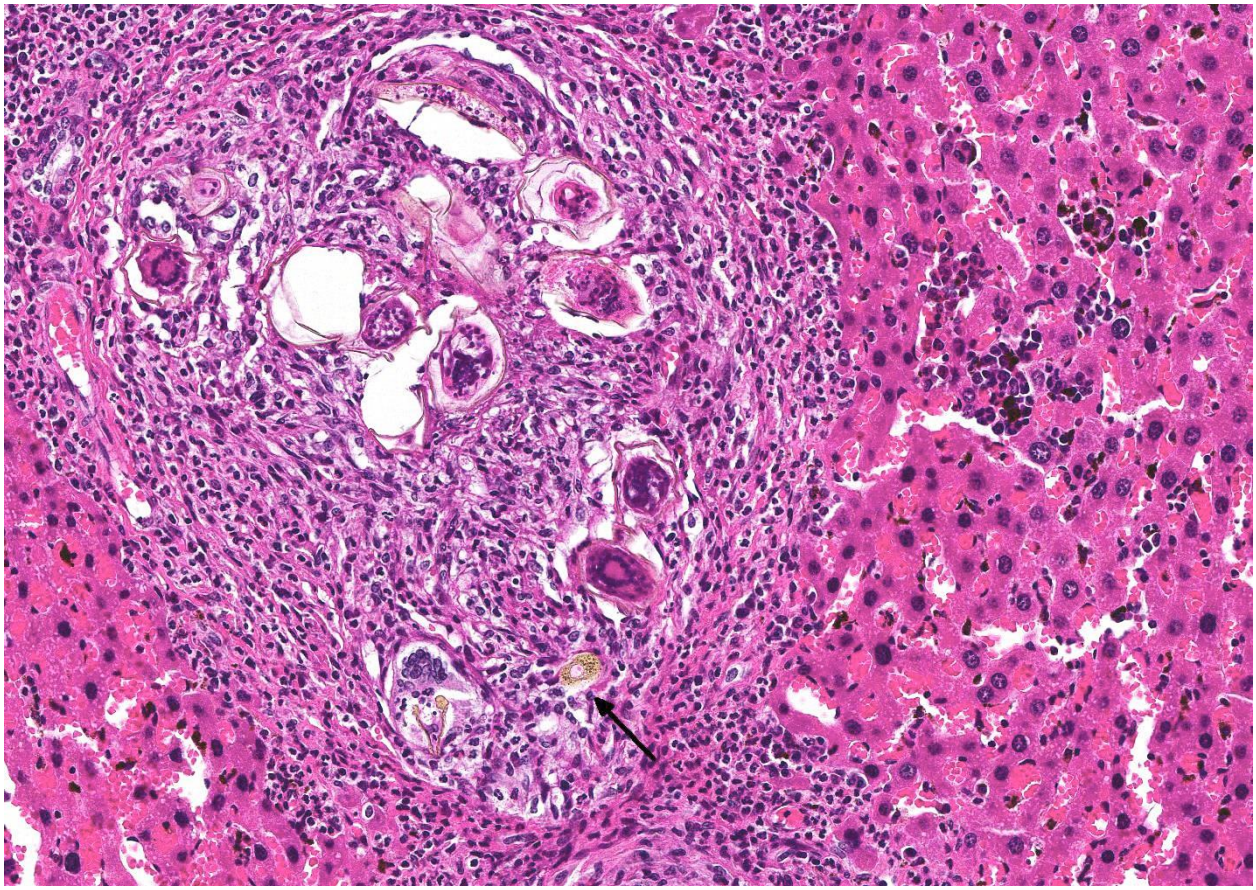

Liver, mouse. Granulomas are centered on numerous schostosome eggs with a refractile brown shell, which contain a multinucleated miracidium. Cross sections of the ends of eggs are brownish yellow (arrow). The surrounding hepatic parenchyma contains numerous hypertrophic Kupffer cells which often contain brownish granular pigment (hemozoin). There is a focus of extramedullary hematopoiesis within the liver parenchyma at right. (HE, 114X)

The male will then anchor the pair to the mesenteric venules by its powerful suckers and muscular body. Females can produce up to 300 embryonated eggs/day, each containing a miracidium. Eggs are released vessel walls, penetrating via egg-released enzymes, and/or by the host' own immune response (granuloma formation), resulting in intestinal tract entry. Many eggs do not enter the vasculature and end up in tissues eliciting an inflammatory response; if they enter the intestine, they are shed in the feces.

In fresh water, the egg shell ruptures, releasing motile, multiciliated miracidia, which have approximately 12 hours to find a snail host. Once inside the snail, they lose their cilia and transform into a primary sporocyst – a sac-like, asexual breeding chamber with numerous secondary sporocysts. . After approximately 2 weeks, the secondary sporocysts escape the primary sporocyst, and migrate to the snail's hepatopancreas and gonads. After another 2 weeks, secondary sporocysts give rise to thousands of cercariae. Once fully developed, the cercariae emerge from the secondary sporocysts, migrate to the anterior of the snail, and are released into the surrounding water to repeat the life cycle. [4].

Schistosomiasis is the condition in which parasitic eggs lodge in the tissues of the definitive host and elicit an chronic inflammatory response. In humans, eggs can

also lodge in the intestinal mucosa and/or submucosa leading to the formation of granulomatous pseudopapillomas or pseudo-polyps which can cause luminal obstruction, ulceration and/or hemorrhage. [2,3,5,7]. Eggs trapped in pre-sinusoidal portal venules secrete soluble egg antigens which are taken up by antigen presenting cells.

Antigen presentation stimulates Th1 cells to secrete IL-2, IFN-gamma and TNF which in turn ilicit a cell mediated response. As the granuloma becomes more organized, Th1 cells are replaced by Th2 cells which produce IL-4, IL-5, IL-10, and IL-13, and the synthesis of IgE, completing granuloma maturation. As the lesions persist, fibroblasts are stimulated by egg products and T-cell cytokines, and produce collagen. Over time, there is downregulation of the Th2 response, resulting in the reduction in the size of newly-formed granulomas. This immunomodulation may be driven by cytokines IL-10 and TGF-beta, induce T-regulatory cells and regulate Th1/Th2 responses. T-regulatory cells and B cells are known sources of IL-10, a key regulator of the egg induced granulofibrotic response.

Marked eosinophilia is a common feature of acute schistosomiasis and may occur before egg deposition. The migration of eosinophils from the circulation to site of infection is primarily induced by CCL11. Under the influence of the Th2 response, the combined effect of IL-5 and GM-CSF contribute to increase in eosinophilia.

Hepatic stellate cells (HSC) are one of the main sources of collagen in the liver and play a crucial role in schistosome-induced fibrogenesis. When activated by IL-13, they differentiate into myofibroblasts, producing collagen. Chemokines associated with HSC recruitment include CXCL1, CCL7, CCL12, and CCL21. Schistosome eggs can inhibit the differentiation of HSC into myo-fibroblasts; *S. mansoni* has the ability to reverse HSC differentiation to their quiescent state[1].

Chronic schistosomiasis leads to extensive periportal fibrosis, a condition known as Symmer's pipestem fibrosis. Portal fibrosis leads to portal hypertension which contributes to splenomegaly, and esophageal and gastric varices[5,7]. Exsanguination by esophageal variceal bleeds is the major cause of death in humans[7].

JPC Diagnosis: Liver: Hepatitis, granulomatous and eosinophilic, random to portal, with numerous schistosome eggs and moderate intrahistiocytic fluke excrement, Swiss Webster (*Mus musculus)*, mouse.

Conference Comment: Schistosomiasis, a fluke infection utilizing snails as intermediate hosts, is prevalent in domestic animals in Asia, Africa, and tropical areas; interestingly this condition does not often cause clinical disease. Generally, damage caused by flukes is due to the orientation of adults and eggs within the vasculature of the liver; lungs, gastrointestinal tract, urinary tract, and nasal cavity. The schistosome's life cycle is similar to other flukes and outlined nicely by the contributor.

Heterobilharzia americana causes clinical disease in dogs, particularly in the southern United States (Louisiana and Texas). The raccoon serves as the definitive host, while dogs and a multitude of other species (bobcat, armadillo, Brazilian tapir, beaver, coyote, mountain lion, mink, nutria, opossum, red wolf, swamp rabbit, and white-tailed deer) serve as accidental hosts. *H. americana* causes hepatic granulomatous lesions which may result in a variety of clinical signs including: mucoid to bloody diarrhea, lethargy, weight loss, vomiting,

anorexia, and ascites. In some cases, dogs experience hypercalcemia due to release of 1,25-dihydroxycholecalciferol from macrophages resulting from the chronic inflammatory process. Microscopically, liver lesions are characterized by multifocal lymphoplasmacytic, eosinophilic to granulomatous inflammation surrounding mineralized eggs that are often arranged in linear arrays. PCR is required to differentiate *H. americana* from other schistosomes by identification of specific subunit ribosomal RNA.[6]

In this case, the species of *Schistosoma* is unknown. Dr. Chris Gardiner, Consultant for Veterinary Parasitology, Joint Pathology Center, reviewed the case and was also unable to specify which type.

There was spirited discussion during the conference about what to call the brown granular pigment within Kupffer cells. It is a fluke byproduct which may represent blood pigment, fluke excrement, or a combination of both.

Contributing Institution:
Veterinary Pathology
Division of Veterinary Resources
Office of Research Services
National Institutes of Health
https://www.ors.od.nih.gov/sr/dvr/drs/Pages/default.aspx

References:

1. Chuah C, Jones MK, Burke ML, McMannus DP, Gobert GN. Cellular and chemokine-mediated regulation in schistosome-induced hepatic pathology. *Trends Parasitol*. 2014;30(3):141-150.
2. Colley DG, Bustinduy AL, Secor WE, King CH. Human schistosomiasis. *Lancet.* 2014:383:2253-2264.
3. Elbaz T, Esmat G. Hepatic and intestinal schistosomiasis: review. *J Adv Res*. 2013:4:445-452.
4. Lewis FA, Tucker MS. Schistosomiasis. In: Toledo R, Fried B, eds. *Digenetic Trematodes, Advances in Experimental Medicine and Biology*. New York, NY: Springer Science+Business Media; 2014:47-75.
5. Olveda DU, Olveda RM, McManus DP, Cai P, et al. The chronic enteropathogenic disease schistosomiasis. *Int J Infect Dis.* 2014; 28:193-203.
6. Robinson WF, Robinson NA. Cardiovascular system. In: Maxie MG, ed. *Jubb, Kennedy, and Palmer's Pathology of Domestic Animals*. Vol. 3. 6th ed. St. Louis, MO: Elsevier; 2017: 91-94.
7. Shaker Y, Samy N, Ashour E. Hepatobiliary schistosomiasis. *J Clinic Transl Hepatol*. 2014;2:212-216.

CASE IV: MS17-3649 (JPC 4104252).

Signalment: 3-month-old, male and female, AG129, *Mus musculus*, mouse.

History: Mice received one foot pad injection of Zika virus. Seven to ten days later, the mice were submitted to necropsy due to weight loss or having been found dead. At presentation, live mice were scruffy, some were unstable on their rear legs and others had developed hind limb paralysis. The animals were in thin - lean body condition with variable hydration status.

Cerebrum, mouse. 4 sections of brain, from rhinencephalon (left) to cerebellar vermis (right) are presented for examination. (HE, 5X)

Gross Pathology: No gross lesions were present.

Laboratory results: None submitted.

Microscopic Description: Inflammatory changes in the brain were present primarily in the cerebrum and were composed of multifocal, random aggregates of neutrophils, necrotic cells [presumed to be astrocytes] with minimal gliosis. Inflammation varied from minimal - mild and occasionally there were solitary necrotic cells without associated inflammation or interstitial change. Neuronal necrosis varied from none to foci of necrotic neurons. Few vessels had smooth muscle hypertrophy with acute – subacute vasculitis. There was variable ependymal cell necrosis. Similar inflammatory and vascular changes were present in the spinal cord. Some sections of cerebellum had mild granular layer necrosis. Purkinje cells appeared to be spared.

There is variation of the severity of the lesions in some slides.

Acute orchitis with seminiferous tubule cell necrosis was the only other microscopic lesion. [Not submitted]

Transmission Electron Microscopy: In the cytoplasm of cerebral axons and dendrites, there were areas with highly expanded and convoluted endoplasmic reticulum (Image #48). Within the endoplasmic reticulum, there were membrane-bound vesicles with numerous unenveloped, 35- 45 nm, round, dark cored particles. Some virions were heavily clustered while others were widely dispersed within the vesicle. There was adjacent cellular debris with a few degenerated mitochondria. (Image #91) The adjacent tissue was unaffected. (Image #55). Bar = 500 nm.

Contributor's Morphologic Diagnosis: Meningoencephalitis and myelitis, multifocal, minimal to moderate, subacute with neuronal necrosis and vasculitis.

Contributor's Comment: Zika virus is an 11 kb ssRNA Flaviviridae carried by *Aedes* spp. mosquitoes. Other flaviviruses to which it is related are West Nile, Dengue, and yellow fever. Zika virus infection was first described in 1952 where it was isolated from a febrile sentinel rhesus macaque in the Zika forest of Uganda.[3] Since then, the virus has spread to Asia and caused outbreaks in Micronesia in 2007 and French Polynesia in 2013. In 2015, the first case was reported in Brazil.[4,7] Since then, there has been widespread infection, 440,000 – 1.3 million, reported in Central and South America, the

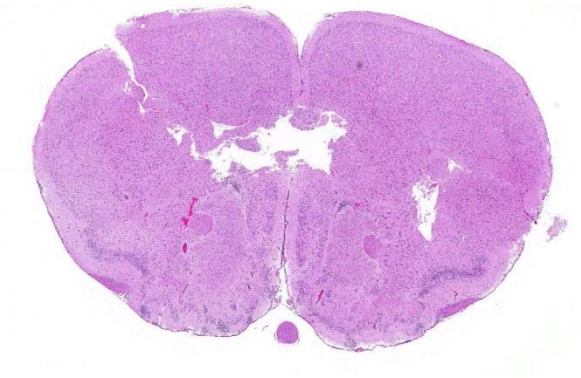

Brain, mouse. The rhinencephalon shows marked hypercellularity within the neuropil, particularly in the ventral regions. (HE, 18X)

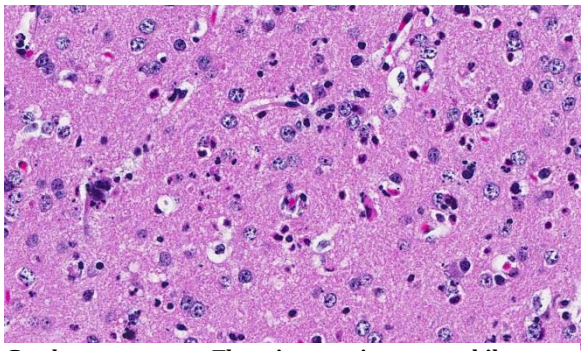

Cerebrum, mouse. There is extensive neutrophil infiltration of the parenchyma throughout the brain, which is most severe in the rhinencephalon. Neutrophils both individually and in small clusters undergo degeneration ad necrosis. (HE, 400X)

Caribbean, and Miami.[2,5,8] The Ministry of Health of Brazil has reported there has been a 20-fold increase in microcephaly.[6]

Infection via Aedes spp. mosquitoes is the most common route of infection. Viral replication occurs within mosquitos which, when taking a blood meal, then infect humans. Nonhuman primates and other mammals may serve as reservoir hosts. Aedes' range is global but most species are concentrated in tropical and subtropical areas. The virus can also be transmitted as a congenital/perinatal or sexual infection. [6,7,8] Transmission via blood transfusion also has been reported.[7]

It is thought that after a mosquito bite, the virus enters through fibroblasts, keratinocytes and immature dendritic cells, migrates to lymph nodes and blood.[8] Once in the cell, the virus induces marked proliferation of the endoplasmic reticulum, rearrangement of the ER membranes, and formation of vesicles, typical of flaviruses. The virus then replicates within the vesicles to form immature virions. The vesicle passes into the Golgi apparatus, becomes glycosylated in and then, being released from it, undergoes final maturation in cytoplasmic vesicles and is released as a mature virion.[7]

Approximately 80% of Zika virus infections are asymptomatic. Infection may be associated with fever, rash, arthralgia, myalgia, headache and conjunctivitis and signs tend to resolve in 2 weeks.[4,6,7] Similar symptoms can also be seen Dengue and Chikungunya virus infection. Individuals may go on to develop meningitis and meningoencephalitis. Additional reported sequelae include hearing loss, hema-tospermia, hypotension and genitourinary symptoms. Infection in Asia and the Americas has been associated with an increase in Guillain-Barré syndrome. Death is not common but has been reported in debilitated/immune-suppressed individuals.[2,8]

Tests to detect Zika can be performed on: CSF, blood, serum, amniotic fluid, fetal and placental tissues, urine, and saliva. During the acute phase of infection, RT-PCR is the best test in which to confirm for Zika virus. However, the period that RNA is present may be as short as 5 days. Serology may also be used but results may be confounded by previous flaviviral infection and time between infection and testing.[8]

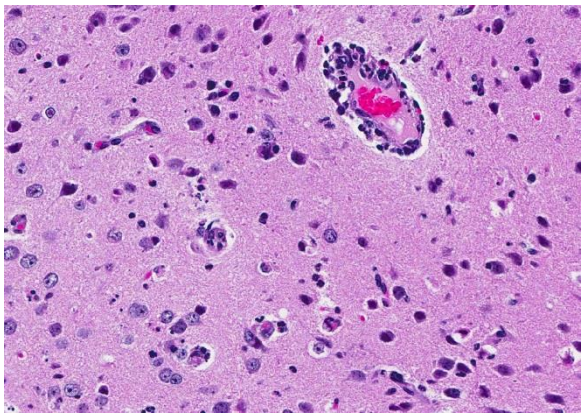

Cerebrum, mouse. In areas of necrosis, vessel walls often contain neutrophils and cell debris (vasculitis). (HE, 400X)

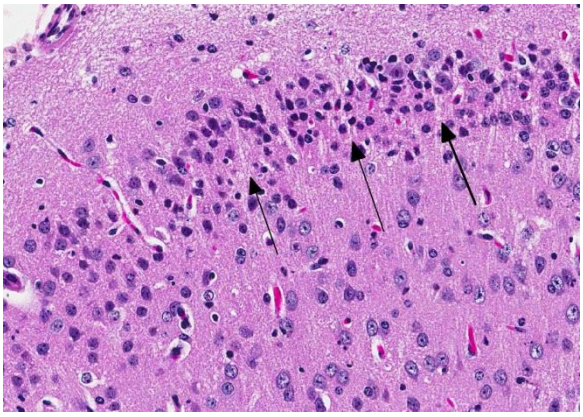

Cerebrum, mouse. There is necrosis of neurons within the cerebrum; in the submeningeal grey matter, it is segmental (arrows). (HE, 400X)

Autopsy findings in a small cohort of ten term neonates included low brain weight, microcephaly with thinning of cerebral cortices with overlapping sutures, pachygyria or agyria and increased ventricle size; thin corpus callosum and optic chiasm; thickening of the leptomeninges; and calcifications between grey and white matter. Other findings included aqueduct stenosis, cerebellar hypoplasia, brainstem abnormalities, and thin, distorted spinal cords. All the neonates had arthrogryposis and some were microphthalmic.[2] Infectious agents that are known to cause similar lesions in infants: intrauterine growth restriction, microcephaly and calcifications, conjunctivitis, hearing loss, rash, hepatosplenomegaly, or thrombocytopenia, are known by the acronym TORCH: Toxoplasmosis, Other (syphilis, varicella-zoster, parvovirus B19, HIV), Rubella, Cytomegalovirus (CMV), and Herpes.

Microscopic lesions appeared to be secondary to abnormal migration and cerebral neuronal/glial loss. Neurons were seen in abnormal locations, as immature cell aggregates around the ventricles, with astrocytosis and calcification. Myelin fibers were decreased or absent. Axonal changes included degeneration, spheroid formation, and loss of orientation. Branching tubes replaced the normal aqueduct. The spinal cord was small due to small cortico-spinal tracts with nerve cell degeneration, loss, gliosis and calcification. Dorsal root ganglia were preserved but ventral ganglia were not. Inflammation was not a prominent feature and when seen, was composed of lymphocytic meningitis, perivascular cuffing and histiocytes and gliosis. Electron microscopy revealed numerous intra-vesicular virions. Muscle atrophy, mild hepatitis and pituitary, retinal and lens mineralization rarely were seen.

Placentas were small for gestational age with inflammation of the villi, fetal membranes and decidua, stromal fibrosis, smooth muscle hyperplasia of villous vessels, chorionic vasculitis, increased vascularity and stromal calcification. In this study, maternal infection in the first or early second trimester led to more severe congenital anomalies.[2]

Until recently, mouse models of Zika have been few. Wild type B6, CD-1, BALB/C mice tend be resistant to Zika infection. However, they can be made to be

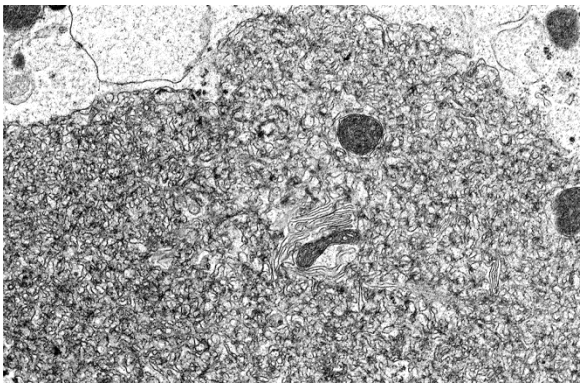

Cerebrum, mouse. In the cytoplasm of cerebral axons and dendrites, there were areas with highly expanded and convoluted endoplasmic reticulum. (Photo courtesy of: Veterinary Pathology, Division of Veterinary Resources, Office of Research Services, National Institutes of Health, https://www.ors.od.nih.gov/sr/dvr/drs/Pages/default.aspx)

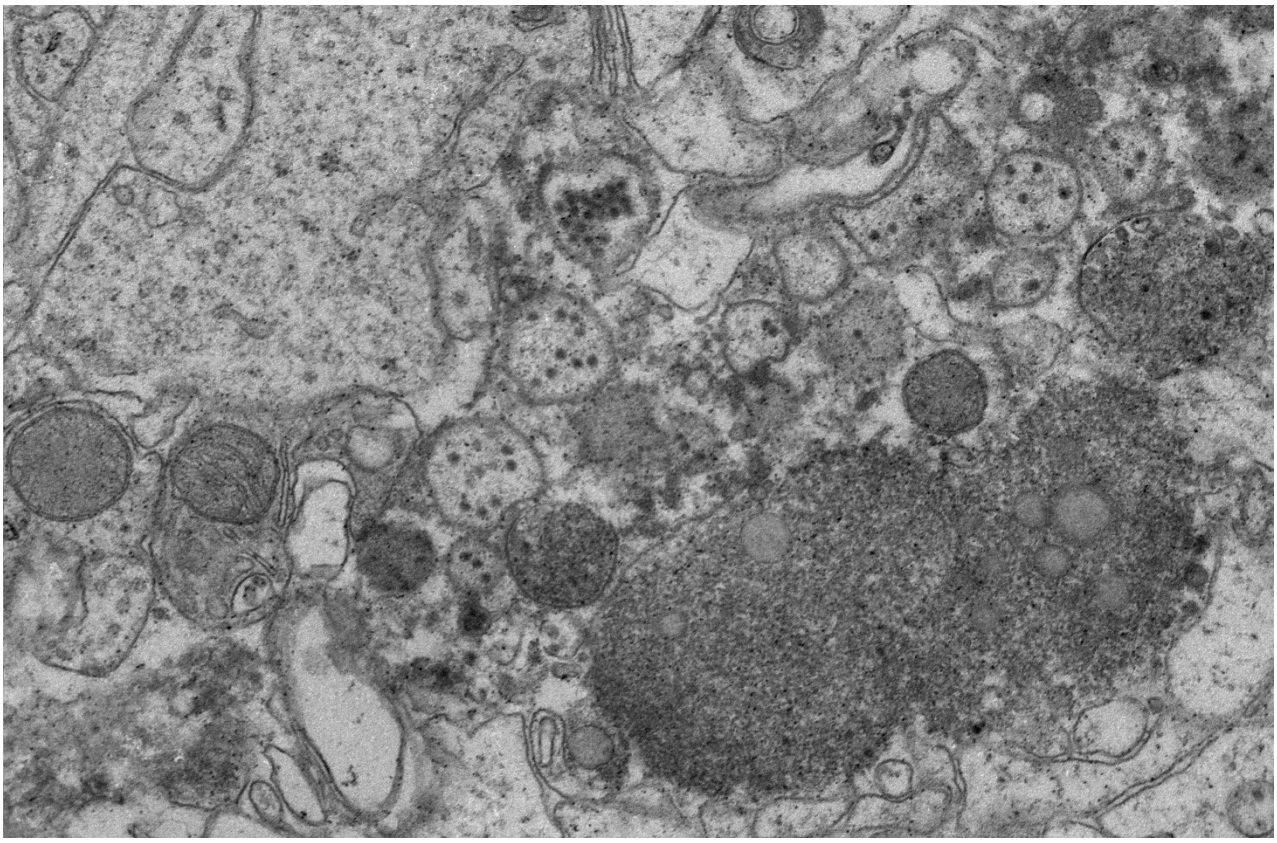

Cerebrum, mouse: Within the endoplasmic reticulum, there were membrane-bound vesicles with numerous non-enveloped, 35- 45 nm, round, dark cored particles. Some virions were heavily clustered while others were widely dispersed within the vesicle. There was adjacent cellular debris with a few degenerated mitochondria. (Photo courtesy of: Veterinary Pathology, Division of Veterinary Resources, Office of Research Services, National Institutes of Health, https://www.ors.od.nih.gov/sr/dvr/drs/Pages/default.aspx)

susceptible by treatment with steroids or mAbs directed against interferon α/β receptors.[5] AG129 mice lack interferon α/β and γ receptors and A129 mice (lacking interferon α/β receptor) are susceptible to Zika infection. As seen in our mice, AG129 mice develop neurologic signs, weight loss and subsequently die but have no gross lesions. Microscopic lesions were limited to the CNS[1]. In some studies, the testis is also affected.[5] The mice have high viral loads are found in brain, spinal cord, spleen and testes and may be studied to determine the pathogenesis of viral dissemination.[5]

JPC Diagnosis: Brain, multiple levels: Meningoencephalitis, necrotizing and neutrophilic, diffuse, moderate with marked neuronal and glial necrosis, AG129 (*Mus musculus*), mouse.

Conference Comment: The conference moderator, who also submitted the case, reviewed the key clinical, gross, and microscopic features of Zika virus (see contributor's comment above). Conference attendees noted necrotic cells randomly arranged throughout the submitted samples (no spinal cord was included) and aggregates of viable and degenerate neutrophils and necrotic cellular debris. Cells are so shrunken it is difficult to determine cell type but most attendees suspect the majority of necrotic cells are

glial cells. The conference moderator showed images from additional tissues including spinal cord and testis. Both of which had a remarkable infiltration of neutrophils and associated necrosis. Within the testis the interstitial space is expanded up to 4 times by neutrophilic inflammation and the spinal cord has degenerative neurons, neuronal necrosis, and spongiosis predominately within the grey matter. There are also numerous astrocytes and neurons that contain eosinophilic intranuclear inclusions, attendees assumed they were viral inclusions. Transmission electron microscopy (TEM) images were provided that clearly identified virions within the cytoplasm but not within the nucleus of affected cells. The pink material seen microscopically cannot be accounted for yet and will most likely be the subject of continued investigation.

Contributing Institution:
Veterinary Pathology
Division of Veterinary Resources
Office of Research Services
National Institutes of Health
https://www.ors.od.nih.gov/sr/dvr/drs/Pages/default.aspx

References:

1. Aliota MT, Caine EA, Walker EC, Larkin KE, Camacho E, Osorio JE. Characterization of lethal Zika virus infection in AG129 mice. *PLoS Negl Trop Dis*. 2016; 10(4):19.
2. Chimelli L, Melo ASO, Avvad-Portari E, Wiley CA, et al. The spectrum of neuropathological changes associated with congenital Zika virus infection. *Acta Neuropathol*. 2017;133(6):983-999.
3. Dick, GW. Zika virus. II. Pathogenicity and physical properties. *Trans R Soc Trop Med Hyg*. 1952;46(5):521-34.
4. Driggers RW, Ho CY, Korhonen EM, Kuivanen S, et al. Zika virus infection with prolonged maternal viremia and fetal brain abnormalities. *N Engl J Med*. 2016;374(22):2142-2151.
5. Morrison, TE, Diamond, MS. Animal models of Zika virus infection, pathogenesis, and immunity. *J Virol*. 2017;91(8):29.
6. Mlakar J, Korva M, Tul N, Popović M, et al. Zika virus associated with microcephaly. *N Engl J Med*. 2016;374(10):951-958.
7. Offerdahl DK, Dorward DW, Hansen BT, Bloom ME. Cytoarchitecture of Zika virus infection in human neuroblastoma and Aedes albopictus cell lines. *Virology*. 2017;501:54-62.
8. Plourde AR, Bloch EM. A literature review of Zika virus. *Emerg Infect Dis*. 2016;22(7):1185-1192.